Cell-to-cell coordination for the spontaneous cAMP oscillation in *Dictyostelium*

Seido Nagano*
Department of Bioinformatics, Ritsumeikan University, 1-1-1 Nojihigashi, Shiga 525-8577, Japan

Shunsuke Sakurai
Life Science Production Div., NOF Corporation, 5-10 Tokodai, Tsukuba 300-2635, Japan
(Received 9 September 2013; published 10 December 2013)

We propose a new cellular dynamics scheme for the spontaneous cAMP oscillations in *Dictyostelium discoideum*. Our scheme seamlessly integrates both receptor dynamics and G-protein dynamics into our previously developed cellular dynamics scheme. Extensive computer simulation studies based on our new cellular dynamics scheme were conducted in mutant cells to evaluate the molecular network. The validity of our proposed molecular network as well as the controversial PKA-dependent negative feedback mechanism was supported by our simulation studies. Spontaneous cAMP oscillations were not observed in a single mutant cell. However, multicellular states of various mutant cells consistently initiated spontaneous cAMP oscillations. Therefore, cell-to-cell coordination via the cAMP receptor is essential for the robust initiation of spontaneous cAMP oscillations.

DOI: 10.1103/PhysRevE.88.062710 PACS number(s): 87.18.Ed, 87.18.Gh, 87.18.Fx, 87.18.Hf

I. INTRODUCTION

There are various types of rhythms in nature that have been utilized by living organisms throughout their evolutionary processes. Rhythms and synchronization of rhythms are involved in the self-regulation of biological systems. A classic example of this is the periodic production of gonadotropin-releasing hormone in mammals [1]. This current study focuses on the cellular slime mold *Dictyostelium discoideum*, which secretes adenosine 3′,5′-monophosphate (cAMP) at a periodicity of 5–10 min in conditions of starvation to control its rate of development. Although the major players in the molecular network that controls the periodic production of cAMP have been previously identified, there is a lack of mathematical modeling studies.

Eukaryotic cells utilize heterotrimeric guanine nucleotide-binding proteins (G proteins) to mediate a vast number of physiological responses. In *Dictyostelium*, four types of cAMP receptors (cAR1, cAR2, cAR3, and cAR4) are G-protein-coupled receptors (GPCRs). The mechanism underlying the coordination between G proteins and various cAMP receptors to control intracellular metabolism and cellular movement remains unclear.

Under conditions of starvation, cAMP is secreted out of the cell where it binds to the cAMP receptor cAR1, which then leads to the activation of adenylyl cyclase (ACA), and finally receptor desensitization. To describe the sustained cAMP oscillation based on this simplified molecular mechanism, Martiel and Goldbeter (MG) [2] proposed an adaptation model that was generalized as a reaction-diffusion scheme [3]. Some of the major caveats of the reaction-diffusion scheme are its dependence on cell density and macroscopic phenomenological theory, as well as its inability to account for individual cell activities. These limitations were overcome using the cellular-dynamics theory [4,5], which incorporated chemotaxis, cell-to-cell interactions, and intracellular molecular mechanisms described by the MG model. The combination of adaptation and cAMP diffusion enables mutual synchronization of cAMP productions between cells and significantly efficient cell aggregation. This synchronization mechanism has been mathematically generalized, thus making it applicable to nonbiological systems [6–9].

Loomis and his colleagues [10,11] proposed molecular networks that successfully reproduced spontaneous cAMP oscillations, but the diffusion equation for cAMP remained undefined. Based on the Laub-Loomis model, Kim *et al*. [12] proposed a multioscillator scheme that coupled cells via the extracellular cAMP (cAMPe) and demonstrated enhanced robustness of the cAMP oscillation. The conclusions made by Kim *et al*. were in agreement with our previous findings [4,5], except for the adopted intracellular molecular mechanisms. It is important to note that there were discrepancies related to cAMPe levels, namely, peaks in cAMPe production were detected before those of intracellular cAMP (cAMPi). This issue was explained by the adoption of a different molecular network in combination with receptor adaptation, which was referred to as the phenomenological adaptation function for cAR1 [13]. On the other hand, Sawai *et al*. [14] derived a different molecular network based on their experimental observations of various mutant cells and their model analyses. As such, the key roles of intracellular phosphodiesterase (RegA) and protein kinase A (PKA) for spontaneous cAMP oscillation, which were originally proposed by Loomis and his collaborators, were questioned. Gregor *et al*. [15] have measured cytosolic cAMP pulses in detail using fluorescence resonance energy transfer (FRET) methods, and the key role of RegA was questioned again.

In order to resolve the conflict regarding the key roles of RegA and PKA for spontaneous cAMP oscillation, we present a new cellular dynamics scheme that incorporates receptor dynamics and G-protein dynamics without a phenomenological function for cAR1 adaptation. Coupling between cAMP receptors and G-proteins for spontaneous cAMP oscillation was previously investigated by Halloy *et al*. [16] and Tang and Othmer [17] using stimulatory G protein Gs and hypothetical

*nagano@sk.ritsumei.ac.jp

inhibitory G protein Gi. While their assumption was not consistent with current experimental findings using *Dictyostelium*, our scheme of G-protein dynamics is consistent with the recent experimental result reported by Janetopoulos *et al.* [18]. Furthermore, this new intracellular molecular network would seamlessly integrate into our previously developed cellular dynamics scheme [4,5] for a study of multicellular states. Spontaneous cAMP oscillation is typically observed in multicellular states, but not in single isolated cells; therefore our new cellular dynamics scheme would be useful for confirming our proposed molecular network, as well as for conclusively determining the roles of RegA and PKA.

II. A MOLECULAR NETWORK FOR SPONTANEOUS CAMP OSCILLATION

In *Dictyostelium discoideum*, cAMP receptors are GPCRs. The binding of cAMPe to the cAMP receptor cAR1 triggers a conformational change in cAR1. This is accompanied by the exchange of GDP for GTP on its G_α subunit followed by the dissociation of the heterotrimeric G protein into G_α and $G_{\beta\gamma}$ subunits. ACA is activated by G_α for cAMP production, and ERK2 is also activated by ligand-bound cAR1. cAMPi activates cAMP-dependent protein kinase A (PKA), which in turn inhibits the mitogen-activated protein kinase (ERK2) and ACA activation, while RegA degrades cAMPi. cAMPi is secreted out of the cell as cAMPe, where it binds to cAR1 or it is degraded by the extracellular phosphodiesterase (PDE).

Receptor dynamics [Eq. (1)] and G-protein dynamics [Eq. (2)] can be written as

$$\mathrm{cAMP}_e + \mathrm{cAR1} \underset{k_{14}}{\overset{k_{13}}{\rightleftarrows}} \mathrm{cAMP}_e\,\mathrm{cAR1} \equiv \mathrm{cAR1}^A, \tag{1}$$

$$\mathrm{G} \underset{k_{16}}{\overset{k_{15}[\mathrm{cAR1}^A]}{\rightleftarrows}} \mathrm{G}_\alpha + \mathrm{G}_{\beta\gamma}. \tag{2}$$

G denotes the inactive G protein, and $\mathrm{cAR1}^A$ is the active, ligand-bound cAR1 receptor. The dissociation constant is defined as $K_d = k_{14}/k_{13}$. Below are the conservation laws for cAR1 [Eq. (3)] and G protein [Eq. (4)], where G_0 and $\mathrm{cAR1}_0$ are the total density of G protein and that of cAR1. It is also assumed that the total number of G proteins is equal to the total number of receptors, and the relationship $[\mathrm{G}_\alpha] = [\mathrm{G}_{\beta\gamma}]$ is maintained:

$$[\mathrm{cAR1}] + [\mathrm{cAR1}^A] = \mathrm{cAR1}_0 = \mathrm{G}_0, \tag{3}$$

$$[\mathrm{G}] + [\mathrm{G}_\alpha] = \mathrm{G}_0. \tag{4}$$

Our scheme is summarized in Fig. 1. Using the above relationships our scheme can be translated into the following coupled equations, where the brackets [ ] stand for concentration:

$$\frac{d[\mathrm{ACA}]}{dt} = k_1[\mathrm{G}_\alpha] - k_2[\mathrm{PKA}][\mathrm{ACA}], \tag{5}$$

$$\frac{d[\mathrm{PKA}]}{dt} = k_3[\mathrm{cAMPi}] - k_4[\mathrm{PKA}], \tag{6}$$

$$\frac{d[\mathrm{ERK2}]}{dt} = k_5[\mathrm{cAR1}^A] - k_6[\mathrm{PKA}][\mathrm{ERK2}], \tag{7}$$

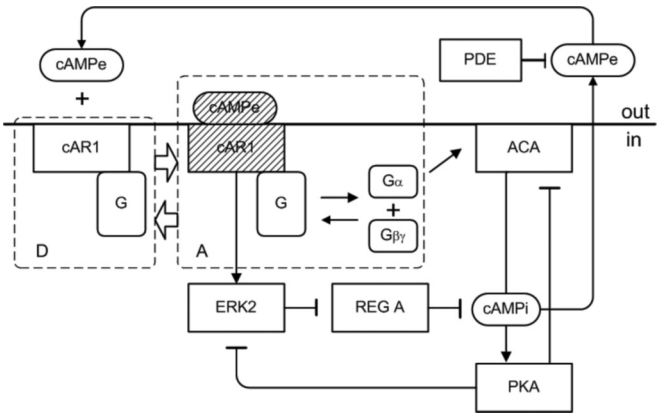

FIG. 1. A molecular network for spontaneous cAMP oscillations and adaptation. Extracellular cAMP (cAMPe) binds cAMP receptors (cAR1), which promotes dissociation of the G_α subunit from the G protein, and G_α activates intracellular cAMP production by ACA. Once the density of G_α is sufficiently increased within the cell, cAMP production is halted, leading to the adaptation and desensitization of the receptors.

$$\frac{d[\mathrm{RegA}]}{dt} = k_7 - k_8[\mathrm{ERK2}][\mathrm{RegA}], \tag{8}$$

$$\frac{d[\mathrm{cAMPi}]}{dt} = k_9[\mathrm{ACA}] - k_{10}[\mathrm{RegA}][\mathrm{cAMPi}], \tag{9}$$

$$\frac{d[\mathrm{cAMPe}]}{dt} = k_{11}[\mathrm{cAMPi}] - k_{12}[\mathrm{cAMPe}], \tag{10}$$

$$\frac{d[\mathrm{cAR1}^A]}{dt} = k_{13}(\mathrm{G}_0 - [\mathrm{cAR1}^A])[\mathrm{cAMPe}] - k_{14}[\mathrm{cAR1}^A], \tag{11}$$

$$\frac{d[\mathrm{G}_\alpha]}{dt} = k_{15}[\mathrm{cAR1}^A](\mathrm{G}_0 - [\mathrm{G}_\alpha]) - k_{16}[\mathrm{G}_\alpha]^2. \tag{12}$$

In Eqs. (11) and (12), we have assumed that only ligand-free cAR1 can bind with cAMP, and only G proteins that exist as heterotrimers can dissociate. In the last term of Eq. (12), the relationship $[\mathrm{G}_\alpha] = [\mathrm{G}_{\beta\gamma}]$ was used. Janetopoulos *et al.* [18] observed a steady increase of G-protein activation that reached a dose-independent steady-state level during continuous stimulation, and the G-protein activation did not decline as long as cAMP receptors were stimulated. Unless there is a constant supply of cAMP from outside, external cAMP density declines because of its degradation by PDE and diffusion. The G-protein dynamics of Eq. (11) are completely consistent with this fluorescence resonance energy transfer (FRET) measurements by Janetopoulos *et al.* [18]. It is also assumed that inhibition works to enhance decay rate. Thus, the decay rates of [ACA], [ERK2], [RegA], and [cAMPi] are defined as k_2[PKA], k_6[PKA], k_8[ERK2], and k_{10}[RegA], respectively.

We show kinetic constants k_j for cAR1 in Table I. We can assume that $1\ \mu\mathrm{M} \lesssim G_0 \lesssim 139\ \mu\mathrm{M}$ [19], where G_0 is at its maximum when the distributions of G proteins and receptors are limited in the lipid bilayer membrane, on the other hand, G_0 is at its minimum when G proteins and receptors are distributed throughout the whole cell. The true value of G_0 can take any

TABLE I. Kinetic constants for cAR1 and the robustness. Here $DOR_j = 1 - \max(\underline{k}_j/k_j, k_j/\overline{k}_j)$ is the degree-of-robustness measure, and the lower and upper limits of the stable oscillation area are given by $\underline{k}_j$ and $\overline{k}_j$, respectively. Robustness increases based on the value of DOR_j. The bifurcation analysis package MATCONT [21] was used.

Parameter	Units	Nominal value	$\underline{k}_j$	$\overline{k}_j$	DOR_j
k_1	min^{-1}	2.3×10^{1}	5.6×10^{0}	3.8×10^{1}	0.39
k_2	$\mu\mathrm{M}^{-1}\mathrm{min}^{-1}$	7.6×10^{0}	3.9×10^{0}	2.2×10^{1}	0.49
k_3	min^{-1}	7.3×10^{-1}	6.2×10^{-1}	1.9×10^{0}	0.15
k_4	min^{-1}	4.8×10^{-1}	0.0×10^{0}	5.0×10^{-1}	0.04
k_5	min^{-1}	2.3×10^{1}	1.0×10^{1}	3.1×10^{1}	0.26
k_6	$\mu\mathrm{M}^{-1}\mathrm{min}^{-1}$	5.4×10^{0}	4.4×10^{0}	1.9×10^{1}	0.19
k_7	$\mu\mathrm{M}\mathrm{min}^{-1}$	4.8×10^{0}	3.8×10^{0}	2.6×10^{1}	0.21
k_8	$\mu\mathrm{M}^{-1}\mathrm{min}^{-1}$	2.3×10^{1}	1.0×10^{1}	3.1×10^{1}	0.26
k_9	min^{-1}	5.2×10^{0}	1.3×10^{0}	8.6×10^{0}	0.40
k_{10}	$\mu\mathrm{M}^{-1}\mathrm{min}^{-1}$	1.6×10^{1}	1.3×10^{1}	8.6×10^{2}	0.19
k_{11}	min^{-1}	8.5×10^{-1}	4.3×10^{-1}	9.7×10^{-1}	0.12
k_{12}	min^{-1}	1.0×10^{1}	9.3×10^{0}	2.8×10^{1}	0.07
k_{13}	$\mu\mathrm{M}^{-1}\mathrm{min}^{-1}$	6.9×10^{0}	3.5×10^{0}	7.8×10^{0}	0.12
k_{14}	min^{-1}	1.2×10^{1}	1.1×10^{1}	3.1×10^{1}	0.08
k_{15}	$\mu\mathrm{M}^{-1}\mathrm{min}^{-1}$	3.5×10^{0}	1.6×10^{0}	7.2×10^{0}	0.51
k_{16}	$\mu\mathrm{M}^{-1}\mathrm{min}^{-1}$	3.0×10^{0}	2.4×10^{0}	$>2.0 \times 10^{2}$	0.20
G_0	$\mu\mathrm{M}$	4.0×10^{0}	3.1×10^{0}	5.4×10^{0}	0.23

value in that range. Figure 2 shows stable cAMP oscillations with the periodicity of approximately 7 min.

III. CELLULAR DYNAMICS FOR AGGREGATION

It is well established that only multicellular clusters of *Dictyostelium* can initiate spontaneous cAMP oscillation. Therefore, we need a multicellular scheme to compare with experimental observations. In 1998 we proposed a theory of diffusion-assisted synchronization [4] to explain efficient *Dictyostelium* aggregation. A subsequent study revealed that the diffusion of a ligand and receptor coupling is critical for the mutual synchronization of cellular metabolism and the robust aggregation of amoebae [6]. Our previous scheme included the intracellular MG model, chemotaxis, and cell-to-cell interaction in a consistent manner. Herein we replace

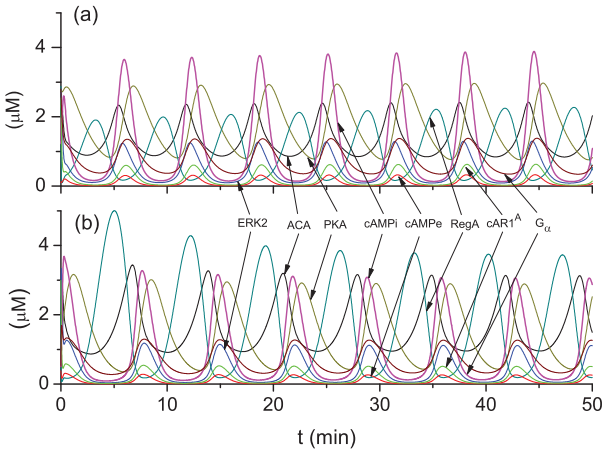

FIG. 2. (Color online) Kinetics of molecular production for cAMP receptor cAR1: (a) a molecular network in Fig. (1), (b) PKA-dependent inhibition of ERK2 is removed from Fig. (1).

the MG model with the current molecular network given by Eqs. (5)–(9), (11), and (12). Furthermore, in order to account for the spatial distribution of cells and the cAMP diffusion, we replace Eq. (10) with

$$\frac{\partial[\mathrm{cAMPe}(\vec{x},t)]}{\partial t} = k_{11}\sum_{j=1}^{N}[\mathrm{cAMPi}(\vec{x},t)]\delta(\vec{x}-\vec{x_j}) - k_{12}[\mathrm{cAMPe}(\vec{x},t)] + D\nabla^2[\mathrm{cAMPe}(\vec{x},t)]. \quad (13)$$

Here $\delta(\vec{x})$ is the two-dimensional δ function, $\vec{x}_j$ are amoeba position vectors, N is the total number of amoebae, and $D = 0.024\ \mathrm{mm}^2/\mathrm{min}$ is the diffusion constant of cAMP. The equations of motion for amoebae become

$$m_a\frac{d^2\vec{x}_j}{dt^2} = \epsilon_2\nabla_j[\mathrm{cAMP}_e(\vec{x}_j,t)] - \sum_{l=1(l\neq j)}^{N}\nabla_j\phi_{m,n}(|\vec{x}_j-\vec{x}_l|) - \eta\frac{d\vec{x}_j}{dt}, \quad (14)$$

where m_a is the mass of an amoeba. On the right-hand side of Eq. (14), the first term is the chemotactic force, the second term is the cell-to-cell interaction force, and the last term is frictional force due to the substrate, and η is the friction coefficient. Additional details are provided by Ref. [4]. This whole scheme allows the comparison of any molecular network with experimental observations. In Fig. 3 we show the aggregation of 127 wild-type cells, where the leak rate of cAMP $k_{11} = 3.5\ \mu\mathrm{M/min}$ [15] was adopted. To determine the onset of spontaneous cAMP oscillation, we measured the levels cAMPi and cAMPe in the central cell of three hexagonal clusters of varying sizes, $N = 7$, $N = 37$, and $N = 61$ (Fig. 4), where the distance between the nearest cells is the cell diameter σ. When $N = 7$, spontaneous cAMP oscillations were not

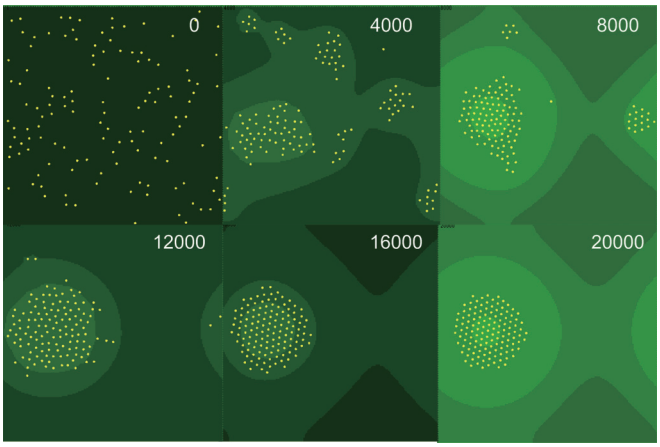

FIG. 3. (Color online) Kinetics of cell aggregates in 127 amoebae in a $30\sigma \times 30\sigma$ area [20], where σ is the diameter of an amoeba and a unit time step is 0.0025 min. Closed circles are *Dictyostelium* amoebae; brighter color in the contour plots shows the higher extracellular cAMP density.

observed [20]. Spontaneous cAMP oscillations were detected when $N = 37$ and 61 [20]; however, sustained oscillation were detectable only when $N = 61$. Based on these findings, there appears to be a threshold number of cells N_c for sustained spontaneous cAMP oscillations. There is a tendency that the value of N_c becomes larger as k_{11} value decreases. Namely, more diffusion of cAMP from bystander cells is necessary to maintain self-sustained spontaneous cAMP oscillation when the leak rate k_{11} is smaller. It is also important to note that the cAMP oscillation stops when the number of cells is greatly increased, and the amount of binding cAMP is increased beyond some critical value. This is achieved by the synchronization of cAMP oscillation [4,5]. In this simulation study, mutual synchronization between cells was quickly achieved although random initial conditions were adopted.

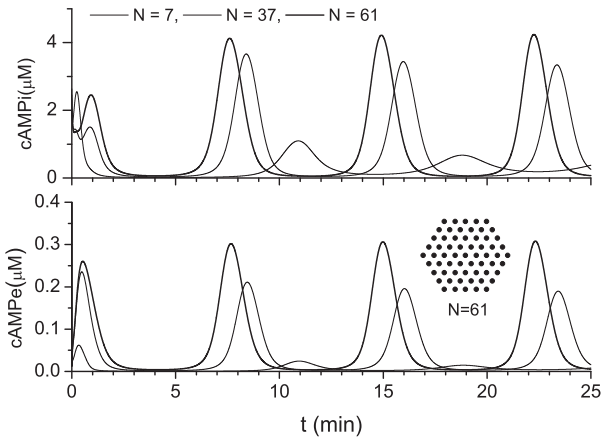

FIG. 4. Requirement of a threshold number of cells for the sustained spontaneous cAMP oscillations. Spontaneous cAMP oscillations were not evident in small hexagonal clusters ($N = 7$) [20]. As the size of a hexagonal cluster increased ($N = 37$), pulsatile cAMP oscillations were detected, but the amplitude gradually decayed with time [20]. Stable pulsatile cAMP oscillations were evident with larger hexagonal clusters ($N = 61$) [20]. Here cAMP leak rate $k_{11} = 3.5\ \mu$M/min was used.

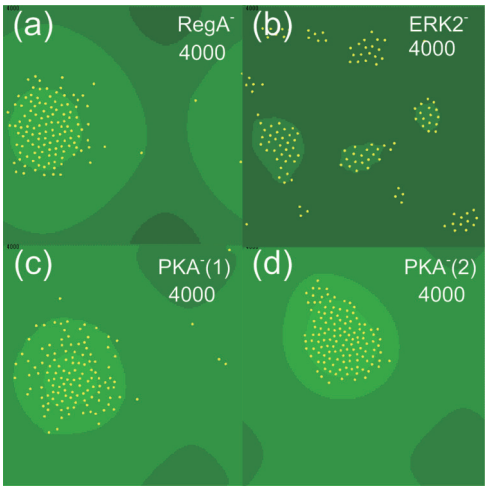

FIG. 5. (Color online) Representative images of aggregation of 127 mutant cells in a $30\sigma \times 30\sigma$ area, over 4000 time steps at interval of 0.0025 min. (a) RegA$^-$: RegA mutant, (b) ERK2$^-$:ERK2 mutant, (c) PKA$^-$(1): PKA mutant (1), (d) PKA$^-$(2): PKA mutant (2). See the main text for the details.

IV. COMPARISON WITH EXPERIMENTS

Changes in aggregation patterns and cAMP pulses are often used to confirm the validity of proposed intracellular molecular networks. Thus, we investigated these factors using our current cellular dynamics scheme. In previous studies, Sawai *et al.* [14] questioned the PKA-dependent inhibitions originally proposed by Maeda *et al.* [11]. We specifically investigated the properties of aggregation and cAMP signaling of (a) RegA mutant RegA$^-$: the production rate of RegA was reduced by setting $k_7 \to k_7/5$; (b) ERK2 mutant ERK2$^-$: the production rate of ERK2 was reduced by setting $k_5 \to k_5/5$; (c) PKA mutant PKA$^-$(1): the negative feedback was reduced by setting $k_2 \to k_2/5$, and $k_6 \to k_6/5$; and (d) PKA mutant PKA$^-$(2): the active rate of PKA was reduced by setting $k_3 \to k_3/5$.

In Fig. 5 we show images of the aggregation of the 127 mutant cells using a time step of 4000 and unit time step of 0.0025 min. The aggregation of wild-type cells at 4000 steps (see Fig. 3) is far from completion; however, RegA mutant cells and PKA mutant cells were closer to the completion of aggregation at 4000 steps. On the other hand, ERK2 mutant cells show an early aggregation pattern. To clarify the mechanism underlying these differences, we measured the amount of time needed for the development of cAMPe at the center cell of 37 hexagonal cell clusters (Fig. 6). The mutant cells oscillated with a time period of approximately 7 min, and none of the isolated single cells sustained clear oscillations. Thus, cell-to-cell coupling via cAR1 is required for the surge of cAMP oscillation. Furthermore, compared to a wild-type cell cluster, RegA mutant cell clusters and PKA mutant cell clusters showed enhanced oscillatory cAMP secretion. Because of such a character, aggregation of these mutant cells begins ahead of wild-type cells. On the other hand, the ERK2 mutant cell cluster showed extremely reduced oscillatory cAMP secretion and very slow aggregation. Furthermore, oscillatory cAMP production by RegA mutant and PKA mutant cells ceased upon aggregation in the $N = 127$, but wild-type cells maintained

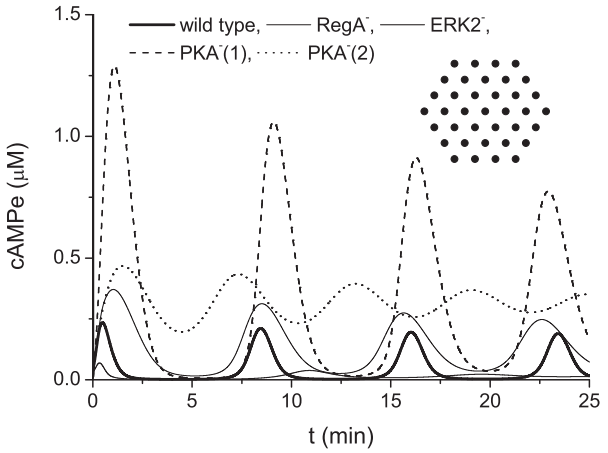

FIG. 6. Kinetics of cAMPe production in the central cell of a 37-cell cluster. RegA mutant cells and PKA mutant cells produce cAMP pulses with larger amplitude compared to wild-type cells. On the other hand, ERK2 mutant cells produce extremely small cAMP, although oscillations can be found.

oscillatory cAMP production even after the completion of aggregation (Fig. 3). Therefore, in accordance with a previous report by Sawai *et al.* [14], the cellular aggregates of RegA mutants and PKA mutants cannot grow as large as that of wild-type cells.

V. PKA-DEPENDENT INHIBITION OF ERK2

PKA-dependent inhibition of ACA was necessary for our scheme to be consistent with previous observations [14]. However, surprisingly PKA-dependent inhibition of ERK2 did not play a significant role in our analysis. As a matter of fact, we can obtain similar results by replacing Eq. (7) with

$$\frac{d[\mathrm{ERK2}]}{dt} = k_5[\mathrm{cAR1}^A] - k_6[\mathrm{ERK2}]. \qquad (7')$$

TABLE II. Kinetic constants for Fig. 2(b).

Parameter	Units	Nominal value
k_1	min^{-1}	3.5×10^{1}
k_2	$\mu\mathrm{M}^{-1}\mathrm{min}^{-1}$	1.2×10^{1}
k_3	min^{-1}	1.1×10^{0}
k_4	min^{-1}	7.3×10^{-1}
k_5	min^{-1}	3.5×10^{1}
k_6	$\mu\mathrm{M}^{-1}\mathrm{min}^{-1}$	1.6×10^{1}
k_7	$\mu\mathrm{M}\mathrm{min}^{-1}$	7.3×10^{0}
k_8	$\mu\mathrm{M}^{-1}\mathrm{min}^{-1}$	3.5×10^{1}
k_9	min^{-1}	7.9×10^{0}
k_{10}	$\mu\mathrm{M}^{-1}\mathrm{min}^{-1}$	2.4×10^{1}
k_{11}	min^{-1}	1.3×10^{0}
k_{12}	min^{-1}	1.5×10^{1}
k_{13}	$\mu\mathrm{M}^{-1}\mathrm{min}^{-1}$	1.0×10^{1}
k_{14}	min^{-1}	1.8×10^{1}
k_{15}	$\mu\mathrm{M}^{-1}\mathrm{min}^{-1}$	5.3×10^{0}
k_{16}	$\mu\mathrm{M}^{-1}\mathrm{min}^{-1}$	4.6×10^{0}
G_0	$\mu\mathrm{M}$	4.0×10^{0}

This means that we can remove PKA-dependent inhibition of ERK2 from our molecular network in Fig. 1 without altering the predictive value of our scheme. Figure 2(b) shows numerical results without PKA-dependent inhibition of ERK2. Corresponding kinetic constants are presented in Table II.

VI. DISCUSSION

We have proposed a new cellular dynamics scheme for spontaneous cAMP oscillations without introduction of a phenomenological function for cAR1 adaptation. Furthermore, both experimentally confirmed G-protein dynamics and receptor dynamics have been successfully incorporated into the molecular network. Thus, we have confirmed the validity of our molecular network based on the comparison of the computer simulation model and experimental observations.

Herein we have replaced the intracellular MG model with a new molecular network that is consistent with recent experimental observations. Nonetheless, our study substantiated that the interaction between cells through the receptor-to-cAMPe leads to amplitude and frequency modulation of cAMPi as a key mechanism of aggregation [4,5]. Nonexcitable cells form temporary aggregation centers that become excitable and grow into larger aggregation centers. As the number of cells within the aggregation center increases, there was a qualitative change in the frequency modulation of cAMPi: namely, the cAMPi density approached a quasisteady level that was necessary for the onset of morphogenesis. This process was consistent with our previous cellular dynamics study.

We have adopted a PKA-dependent feedback that was originally proposed by Maeda *et al.* [11]. However, our current model is distinct in a number of ways: (a) cAMPe is formed from the leaked cAMPi instead of being formed directly from ACA, thus cAMPe and cAMPi are not independent variables, (b) both experimentally confirmed G-protein dynamics and ligand-receptor dynamics of cAMP receptors are included, and (c) a multicellular dynamical model instead of a nonmoving single-cell model is used.

Sawai *et al.* [14] questioned the key role of PKA in the spontaneous cAMP oscillation that was originally proposed by Loomis and his collaborators [11]. Our cellular dynamics study showed that the discordance was not evident in the multicellular system although isolated cells failed to produce spontaneous cAMP oscillations. Nonetheless, one key negative feedback mechanism played a critical role in spontaneous cAMP oscillations. As shown in Fig. 2(b), PKA-dependent inhibition of ERK2, but not PKA-dependent inhibition of ACA, was redundant and removable from the molecular network. In order to derive their conclusion, they adopted a rule-based scheme that was originally described by Kessler and Levine [22] that classified mutant waveforms in terms of two parameters β and η. According to this model analysis, cellular automata for the cellular movement and the diffusion equation for cAMP were adopted, and cell excitability was taken into account phenomenologically. In their scheme, there is a difficulty in time keeping the cell position due to the nature of cellular automata. This may reflect the necessity of a 20-fold lower diffusion constant compared to the experimental value. Furthermore, cell excitability was controlled by two parameters β and η. However, this model failed to present a

method to derive any specific molecular network from given values of β and η. Thus, it is not clear whether their scheme incorporated negative feedback of PKA.

We should also highlight the nonlinearity of spontaneous cAMP oscillations. Based on numerous previous experimental observations and our current study, it is clear that spontaneous cAMP oscillations are detectable in clusters of cells, but not from a single isolated cell. This means that intracellular biochemical reactions of every cell are strongly coupled together via cAMP receptors, which is required for the onset of spontaneous cAMP oscillations. Thus, both amplitude and phase of cAMP oscillations significantly vary during the aggregation process, and both of these factors are included in our current scheme. This is in stark contrast to the phase model adopted by Gregor *et al*. [15], which failed to include amplitude variation and which averaged the level of cytosolic cAMP and cell distribution over all cells in their analysis. While these assumptions may be reasonable at low cell densities, such as the very early stage of the aggregation, there is a limitation to using it for the judgment of the validity of the molecular network for the spontaneous cAMP oscillations.

We have investigated the effect of cAMP leak rate k_{11} from 0.8 to 4.0 μM/min. Then the threshold number of cells N_c for sustained spontaneous cAMP oscillations decreased gradually from about 140 to 60 with an increase of k_{11} value. However, general properties discussed in this paper did not change at all. Thus, we have shown only the case of $k_{11} = 3.5$ μM/min here. Gregor *et al*. [15] have derived it by adopting the above-mentioned assumptions. To obtain the value of k_{11} more directly from experiments without any assumption, we have to observe N_c values by changing the number of amoebae confined in a small isolated well. We are conducting such an experiment currently, and we will report more reliable k_{11} values together with corresponding cellular dynamics simulation studies in the near future.

Our new cellular dynamics scheme has successfully reproduced experimental observations. However, our molecular network, chemotaxis, and cell-to-cell communication are still highly simplified compared to the latest experimental findings. Thus, it may not be proper to remove the possible role of gene expression [14] completely as one of the key roles for the spontaneous cAMP oscillation. Further studies are needed to comprehensively address this problem.

ACKNOWLEDGMENT

We appreciate Fukuya Mori and Kazuya Okagawa for carefully reviewing our numerical calculations.

[1] A. Khadra and Y. Li, Biophy. J. **91**, 74 (2006).
[2] J. L. Martiel and A. Goldbeter, Cells. Biophys. J. **52**, 807 (1987).
[3] J. J. Tyson and J. D. Murray, Development **106**, 4216 (1989).
[4] S. Nagano, Phys. Rev. Lett. **80**, 4826 (1998).
[5] S. Nagano, Develop. Growth Differ. **42**, 541 (2000).
[6] S. Nagano, Prog. Theor. Phys. **103**, 229 (2000).
[7] S. Nagano, Prog. Theor. Phys. **107**, 861 (2002).
[8] S. Nagano, Phys. Rev. E **67**, 056215 (2003).
[9] A. Yokoyama and S. Nagano, J. Phys. Soc. Jpn. **77**, 024002 (2008).
[10] M. T. Laub and W. F. Loomis, Mol. Biol. Cell. **9**, 3521 (1998).
[11] M. Maeda, S. Lu, G. Shaulsky, Y. Miyazaki, H. Kuwayama, Y. Tanaka, A. Kuspa, and W. F. Loomis, Science **304**, 875 (2004).
[12] J. Kim, P. Heslop-Harrison, I. Postlethwaite, and D. G. Bates, PLoS Comput. Biol. **3**, e218 (2007).
[13] S. Sakurai and S. Nagano, J. theor. Biol. **307**, 37 (2012).
[14] S. Sawai, P. A. Thomason, and E. C. Cox, Nature (London) **433**, 323 (2005).
[15] T. Gregor, K. Fujimoto, N. Masaki, and S. Sawai, Science **328**, 1021 (2010).
[16] J. Halloy, J. Lauzeral, and A. Goldbeter, Cells Biophys. Chem. **72**, 9 (1998).
[17] Y. Tang and H. G. Othmer, Math. Biosci. **120**, 25 (1994).
[18] C. Janetopoulos, T. Jin, and P. Devreotes, Science **291**, 2408 (2001).
[19] R. L. Johnson, P. J. M. Van Haasrter, A. R. Kimmel, C. L. Saxe III, B. Jastorff, and P. N. Devreotes, J. Biol. Chem. **267**, 4600 (1992).
[20] See Supplemental Material at http://link.aps.org/supplemental/10.1103/PhysRevE.88.062710 for movies.
[21] A. Dhooge, W. Govaerts, and Y. A. Kuznetsov, ACM Trans. Math. Softw. **29**, 141 (2003).
[22] D. A. Kessler and H. Levine, Phys. Rev. E **48**, 4801 (1993).